4.7 DEVELOPMENT FOR A NUDGING ASSIMILATION PROCEDURE OF CLOUD RESOLVING STORM SIMULATOR USING MULTIPARAMETER RADAR DATA

Shingo Shimizu*[1)], Takeshi Maesaka[1)], Ryohei Misumi[1)] • Koyuru Iwanami [1)], Masayuki Maki[1)], Tadashi Yamada[2)], Shuuichi Tsutiya[2)], and Wataru Sato[2)]

1:National Research Institute for Earth Science and Disaster Prevention, Tsukuba, Japan

2: Graduate School of Science and Engineering, Chuo University, Tokyo, Japan.

1. INTRODUCTION

The National Research Institute for Earth Science and Disaster Prevention (NIED) in Japan developed a multiparameter (MP) radar at the X-band wavelength (MP-X) for hydrological and meteorological application (Iwanami et al., 2000). We designed a real-time radar network consisting of multiple MP radars and Doppler radars over Kanto Plain, Japan (Maki et al., 2006). A cooperative observation in the radar network (a MP radar and a Doppler radar) has been started from July in 2006. By the warm season in 2008, 2 MP radars and a Doppler radars will be added in the network. Using the observational data obtained in the radar network, we are trying to develop a real-time assimilation system for a short-range (up to 2 hours) forecast of severe weather.

In this study, a nudging assimilation procedure was developed in cloud-resolving storm simulator (CReSS: Tsuboki and Sakakibara, 2001). A hail storm observed in 15 July 2006 in Kanto Plain was simulated with the nudging assimilation. The sensitivity of various observational parameters to the maintenance of a precipitation system was investigated.

2. OBSERVATIONAL DATA AND ANALYSIS METHOD

A isolated thunderstorm observed over the Kanto plain in Japan on 15 July 2006 was observed in a dual-Doppler radar analysis region (Fig. 1) from 1200 to 1250 Japan Standard Time (JST). MP-X, covering 83 km in radius, recored sets of volume scans of reflectivity, Doppler velocity, differential propagation phase (Φdp), specific differential phase (Kdp), and correlation coefficient (ρhv) every 5 minutes. One volume scan consisted of 13 elevation angles (0.6°, 1.1°, 1.6°, 2.2°, 2.7°, 3.4°, 3.8°, 4.7°, 5.7°, 6.9°, 8.4°, 10.3°, 12.9°). Chuo university (CHUO) radar, covering 80 km in radius, records sets of reflectivity and Doppler velocity every 5 minutes, except for 1210 and 1240 JST. CHUO radar operated volume scan, which consisted of 10 elevation angles (1.0°, 2.0°, 3.5°, 5.5°, 7.0°, 9.0°, 12.0°, 20.0°, 35.0°, 50.0°), at 1220 and 1230 JST. Unfortunately, CHUO radar operated one elevation scan (1.0°) in the other time.

These PPI data were interpolated in a Cartesian coordinate system with a 1-km horizontal grid interval and a 0.25-km vertical interval (CAPPI dataset). For the interpolation, the location of the bin data was shifted to consider the advection (Gal-Chen, 1982) assuming a southeasterly 9 m s^{-1} storm movement, and a Cressman-type weighting function was used. For MP-X radar data, the horizontal and vertical effective radius of influence were 1.5 km and 1.0 km, respectively. For CHUO radar data, larger effective radius were selected (2.0 km in horizontal and 1.5 km in vertical). This made it possible to obtain sufficient continuity of the CAPPI dataset for dual Doppler radar analysis especially below 3 km above sea level (ASL).

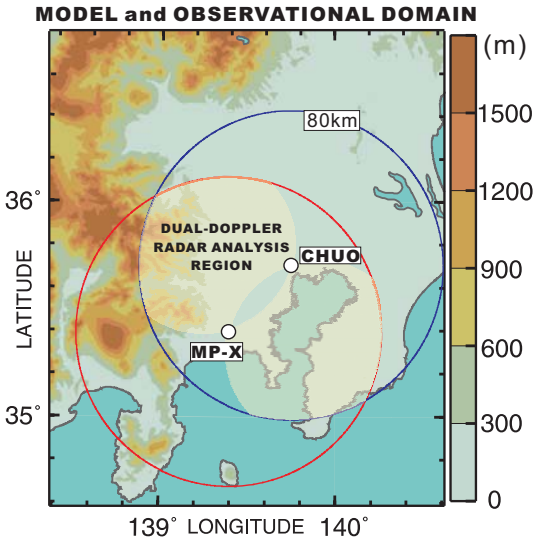

Fig. 1: Model domain (200 km × 240 km) and dual-Doppler radar analysis domain and altitude in the domain. Open circle indicates radar location (MP-X and CHUO). Red and blue circles indicate the observation range of MP-X and CHUO, respectively. Highlighted region indicates dual Doppler radar analysis region.

Three components of wind in the Cartesian coordinate system were calculated within the highlighted region in Fig. 1. We conducted dual-Doppler radar analysis with the upward integration method (Ray et al., 1980) because of the lack of radial velocity data above 3 km in height for CHUO radar. The boundary condition of w = 0 m s^{-1} at z = 0.25 km was employed. It is known that the accuracy of vertical components obtained in the upward integration method is generally low (Chong and Testud, 1983). In this study, we used horizontal components of wind for nudging procedure below 3 km ASL in height. The terminal fall velocities of rain and snow were adapted from Foot and duToit, 1982, and the terminal fall velocity of “graupel and small hail” was

*Corresponding author address: Shingo Shimizu, National Research Institute for Earth Science and Disaster Prevention, Tsukuba, Ibaraki, Japan,306-0005; e-mail: shimizus@bosai.go.jp

adapted from Staraka et al., 2000.

3. MODEL DESCRIPTION AND NUDGING EXPERIMENT

A simulation using CReSS was conducted in 200 $\times$ 240 km $\times$15 km domain with same resolution as the dual Doppler radar analysis. CReSS is a three-dimensional non-hydrostatic model (Tsuboki and Sakakibara, 2002). CReSS uses the quasi-anelastic Navier-Stokes equations and includes a bulk cold rain parameterization and a 1.5-order closure with a turbulent kinematic energy prediction. In the microphysics of CReSS, six species (water vapor, cloud, ice, rain, snow, and graupel) are considered. Their mixing ratio and number concentrations of ice, snow, and graupel are predicted.

Initial and lateral boundary conditions to the CReSS model were provided by outputs of the Japan Meteorological Agency meso scale model (MSM). The MSM contains a horizontal resolution of 10 km with 241 $\times$ 253 grid points and 20 vertical levels. The 1km-CReSS was integrated forward in time using the MSM output data at 12 JST on 15 Jul 2006 as the initial data.

Four nudging experiments using different combinations of observational parameters were compared with control run. The four nudging experiments are (1) nudging of horizontal wind below 3 km ASL (experimental name: UV), (2) nudging of mixing ratio of rain estimated by reflectivity (R), (3) nudging of both horizontal wind below 3 km in height and mixing ratio of rain estimated by reflectivity (Roux, 1985) (UVR), (4) same as (3) except that initial vapor filed in the region where the observed reflectivity was over 0 dBZ was forced to be saturated (UVR-QV0). Integration of CReSS was conducted from 1200 to 1500 JST. Nudging procedure was performed from 12:00 to 12:30 JST.

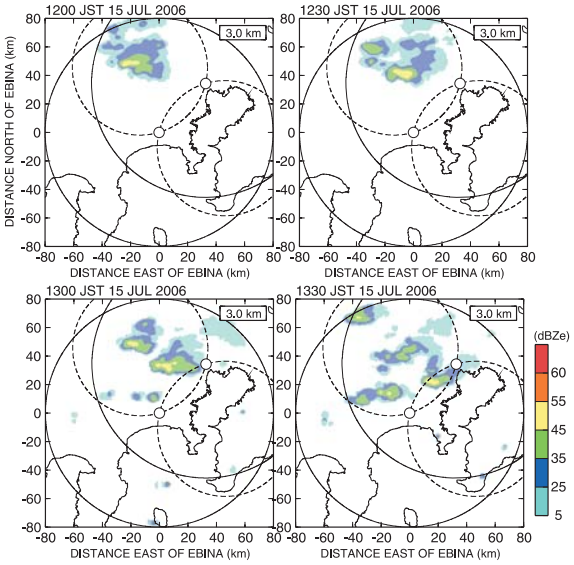

Fig. 2: Reflectivity at a height of 3 km obtained by MP-X radar from 1200 to 1330 JST.

4. RESULTS

An isolated meso-scale convective system (MCS) was observed within the dual Doppler radar observation region from 1140 to 1300 JST in 15 JUL 2006 (Fig. 2). The isolated MCS had a steady hook-shaped reflectivity distribution for more than 90 minutes. The isolated MCS moved southeast-ward at a speed of 25-30 km h^{-1}.

The reflectivity distribution and storm-relative wind derived from dual Doppler radar analysis is shown in Fig. 3. A low-level environmental storm-relative inflow blew from southeast. The inflow became a cyclonic flow around the center of hook-shaped echo at 1205 JST. The maximum vorticity at the center of hook-shaped echo was 4.0 - 5.0 $\times$ 10^{-3} s^{-1} at 2 km ASL from 1205 to 1220 JST.

Reflectivity calculated from mixing ratio of rain using empirical equation (Roux, 1985) and storm-relative horizontal wind at a height of 3 km in control experiment and four experiments from 1230 and 1315 JST were shown in Fig. 4. In the CNTL experiment, hook-shaped distribution of reflectivity and vertical vorticity were not simulated in the radar analysis domain. However, the other four experiments succeeded to simulate single convective cell or vertical vorticity at 1230 JST. In UV experiment, vertical vorticity (4.0 $\times$ 10^{-3} s^{-1}) maintained until 1300 JST, however precipitation disappeared just after 1230 JST. In R experiment, heavy precipitation maintained until 1300 JST, however any vertical vorticity was not simulated. In UVR experiment, heavy precipitation and vertical vorticity were maintained until 1300 JST, however they disappeared around 1310 JST. A new updraft was generated to the south of the dissipating convective cell around 1300 JST (not shown). However, the condensation of vapor did not occur in the new updraft (not shown) because of the lack of lower layer moisture (lifting condensation level was 1 km). In UVR-QV0 experiment, heavy precipitation and vertical vorticity were maintained until 1330 JST. We compared the evaporation cooling rate around the MCS in UVR experiment and UVR-QV0 experiment from 1200 to 1300 JST (not shown). In UVR experiment, larger cooling of rain evaporation in convective region reduced positive buoyancy around initial time. The modification of initial distribution of vapor was most important to the maintenance of precipitation system in this case.

In this study, we used empirical equation for conversion from reflectivity to mixing ratio of rain. The conversion would cause overestimation of mixing ratio of rain because the storm included small hail and graupel (reported from surface observation). In order to estimate more accurate mixing ratio of rain, nudging experiment using the mixing ratio of rain directly estimated from Kdp will be compared with this result.

5. CONCLUSION

A hail storm observed in 15 July 2006 over Kanto Plain, Japan was simulated with nudging assimilation using CReSS. The nudging experiment using horizontal wind velocity below 3 km and mixing ratio of rain estimated from empirical equation (Z-Qr relation) with initial modification of vapor could provide short-range forecast of precipitation region within 1 hour. The nudging experiment using the mixing ratio of rain directly estimated from Kdp will be tested and compared with this result. The mixing ratio of rain directly estimated from Kdp would avoid the overestimation of mixing ratio of rain in CReSS.

References

[1] Chong M. and J. Testud, 1983: Three-dimensional wind field analysis from dual-Doppler radar data. Part III: The boundary condition: An optimum determination based on a variational data., *Mon. Wea. Rev.*, **115**, 670-694,

[2] Foote G. B. and P. S. duToit, 1969: Terminal velocity of raindrops aloft., *J. Appl. Meteorol.*, **8**, 249-253,

[3] Gal-Chen T., 1982: Errors in fixed and moving frame of references: Applications for conventional and Doppler radar analysis. *J. Atmos. Sci.*, **39**, 2279-2300.

[4] Iwanami K. M. Maki, R. Misumi, S. Watanabe, and K. Hata, 2000: The NIED Dual-frequency Cloud Radar System under Development., *Preprints, 29th Conf. on Radar Meteorology*, Montreal, PQ, Canada, Amer. Meteor. Soc., 494-496

[5] Maki, M., K. Iwanami, R. Misumi, T. Maesaka, S. Shimizu, K. Kieda, K. Nakane, A. Kato, K. Dairaku, H. Moriwaki, T. Fukuzono, S. Yazaki, Y. Sasaki, M. Tominaga and T. Nagasaka, 2006: Studies on the Prediction of Landslides and Urban Flooding using an X-Band Multi-Parameter Radar Network, *Second Intn'l Symposium on Quantitative Precipitation Forecasting and Hydrology.*

[6] Ray P. S. and C. L. Ziegler and W. Bumgarner and R. J. Serafin, 1980: Single- and multiple Doppler radar observations of tornadic storms., *Mon. Wea. Rev.*, **108**, 1607-1625,

[7] Roux, F., 1985: Retrieval of thermodynamic fields from multiple-Doppler radar data using the equations of motion and the thermodynamic equation. *Mon. Wea. Rev.*, **113**, 2142-2157,

[8] Straka J. M. and D. S. Zrnic and A. V. Ryzhokov, 2000: Bulk hydrometer classification and quantification using polarimetric radar data: Synthesis of relations., *J. Appl. Meteor.*, **39**, 1341-1372,

[9] Tsuboki K. and A. Sakakibara, 2002: Large-scale parallel computing of Cloud Resolving Storm Simulator., *High Performance Computing, Springer*, H. P. Zima et al. Eds, 243-259

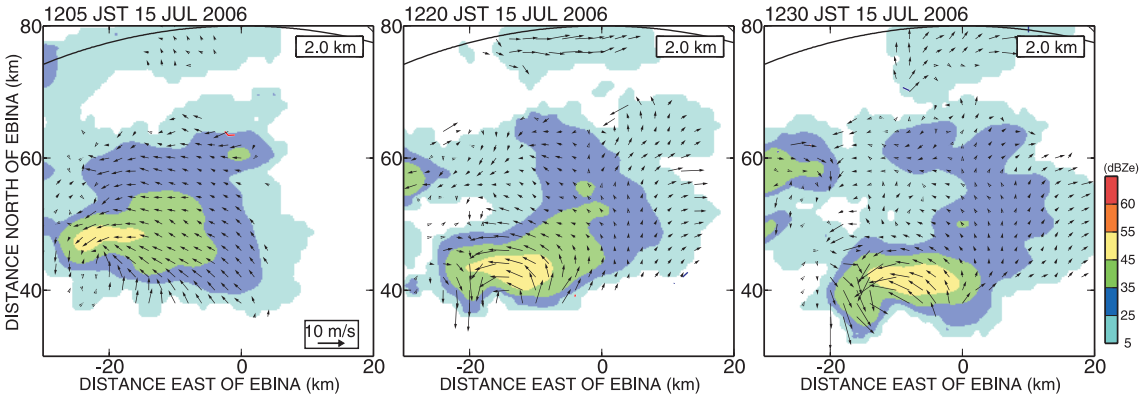

Fig. 3: Storm-relative wind and reflectivity at a height of 2 km obtained by dual-Doppler radar analysis at 1205, 1220, and 1230 JST.

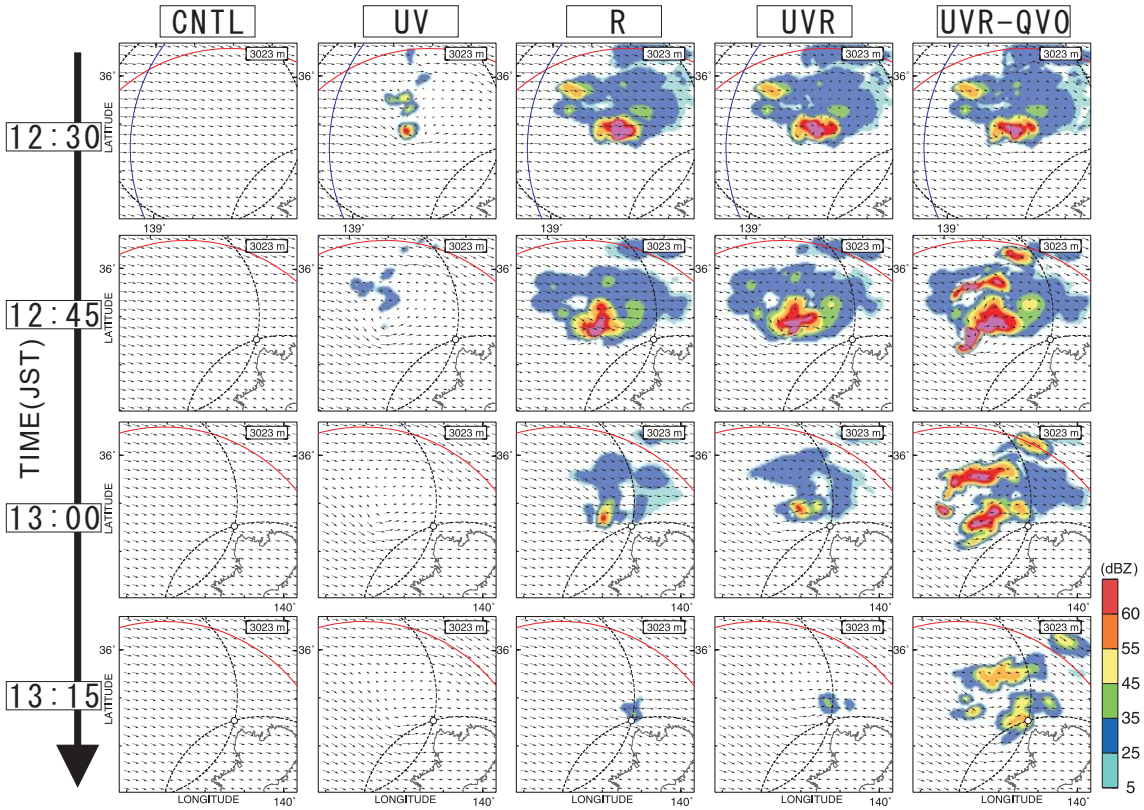

Fig. 4: Reflectivity calculated from mixing ratio of precipitation using empirical equation (Roux,1985) and storm relative wind at a height of 3 km in control experiment (CNTL) and four nudging experiments (UV, R, UVR, UR-QV0)) from 1230 to 1315 JST.